ELSEVIER

Journal of Alloys and Compounds 459 (2008) 209–214

Journal of ALLOYS AND COMPOUNDS

www.elsevier.com/locate/jallcom

Electrodeposition of Zr and electrochemical formation of Mg–Zr alloys from the eutectic LiCl–KCl

Zeng Chen, Milin Zhang *, Wei Han, Xiaolei Wang, Dingxiang Tang

College of Materials Science and Chemical Engineering, Harbin Engineering University, Harbin 150001, PR China

Received 18 March 2007; received in revised form 2 May 2007; accepted 3 May 2007

Abstract

To investigate the electrodeposition mechanism of Zr(IV), the electrochemistry of a LiCl–KCl–K_2ZrF_6 melt at molybdenum and tungsten electrodes was studied at the temperature between 773 K and 973 K. Transient eletrochemical techniques, such as cyclic volatmmetry and chronopotentiometry were used. The results showed that Zr(IV) was reduced to Zr metal by a two-step mechanism corresponding to the Zr(IV)/Zr(II) and Zr(II)/Zr transitions. The intermediate product was identified as $ZrCl_2$ by X-ray diffraction. At a liquid magnesium electrode, Mg–Zr alloy was obtained by potentiostatic electrolysis, and the samples were characterized by scanning electron microscopy and energy dispersive X-ray detector. The zirconium concentration in samples was about 0.8 mass% determined by an inductively coupled plasma atomic emission spectrometer.

Keywords: Electrochemical reactions; Transition metal alloys and compounds; X-ray diffraction

1. Introduction

Zirconium and its alloys are widely used in aviation, metallurgy, atomic energy, chemistry industry and other fields [1]. Moreover, zirconium is a potent grain refiner for magnesium alloys, the unique property has led to the rapid development of zirconium-containing magnesium alloys [2]. At present, the primary methods to prepare zirconium metal and its alloys were thermic reduction methods and molten salt electrolysis methods [3]. However, the thermic reduction process has many disadvantages, the uncontinuity of the production process, more waste in the smelt process, and so on. On the contrary, molten salt electrolysis process is an effective method for the preparation of zirconium and its alloys. Firstly, it could be used to produce the high-melting point metals at low temperature [4–7]. Secondly, the process can be carried out with the simple apparatus. Thirdly, the composition of alloys can be controlled easily.

The technics to produce zirconium metal through molten salt electrolysis had been extensively studied [1,3]. However, as we all know that the exploring of electroreduction mechanism of zirconium is also important for the electrodeposition process. A few studies have been devoted to the electrochemical behaviour of Zr in different molten salt systems. The stand potential Zr(IV)/Zr has been determined in a molten LiCl–KCl eutectic by Baboian et al. [8]. They used zirconium metal as anodic electrode to provide valent ion of Zr and found that the Zr(II) and Zr(IV) could coexist in the molten salts between 450 °C and 550 °C, and the ratio between Zr(II) and Zr(IV) increased with the increasing of temperature. Similar conclusions in the same molten system was made by Suzuki [9] and Kawase and Ito [10]. Basile et al. [11] studied the reduction process of Zr(IV) in the molten NaCl and KCl–LiCl system. They found that Zr(IV) ion was reduced via a four-step reduction mechanism in the molten NaCl melt and two-step in the LiCl–KCl melt. Kipouros and Flengas [12] investigated the oxidation states (+1, +2, +3, +4) of zirconium in alkali metal chloride and fluoride systems over the temperature range 700–750 °C. Sakamura [13] investigated the electrochemical behavior of Zr(IV) in a LiCl–KCl–$ZrCl_4$ melts over the temperature range 450–550 °C. They found that Zr(I) and Zr(II) both appeared in the melt during the electrodeposition of Zr.

This work studied the electroreduction process of Zr(IV) in the molten LiCl–KCl–K_2ZrF_6 system. Zirconium potassium fluoride (K_2ZrF_6) instead of zirconium tetrachloride ($ZrCl_4$) was used as the source of Zr(IV) in the experiment, for the reason that $ZrCl_4$ was easy to sublime at a temperature equal to or above 573 K. Moreover, some work was also done for the preparation

---

* Corresponding author.
E-mail address: milinzhang@126.com (M. Zhang).

0925-8388/$ – see front matter © 2007 Elsevier B.V. All rights reserved.
doi:10.1016/j.jallcom.2007.05.008

of Mg–Zr alloy using the electrochemical methods which has not been reported. Compared to the traditional thermic reduction process, the proposed method could reduce the inclusions, decrease or eliminate the compositional segregation. In addition, the experimental results will be useful for the further study and mass production of Mg–Zr alloy.

Specifically, the experiment was carried out with a solution of K_2ZrF_6 in the eutectic LiCl–KCl at the temperatures between 773 K and 973 K on different substrates: (i) molybdenum wire; (ii) tungsten wire; (iii) liquid magnesium.

2. Experimental

2.1. Cell and electrodes

Fig. 1 shows the experimental apparatus. The primary and secondary crucibles were made of high purity (99.9 wt.%) alumina and quartz, respectively. They were positioned in the graphite outer vessel and heated with the tubular furnace. The temperature measurement was carried out by Chromel–Alumel thermocouple with an accuracy of ±2 K.

The reference electrode was an Ag wire immersed in LiCl–KCl eutectic containing 0.1 mol% AgCl in a Pyrex tube provided with a diaphragm at the bottom. The inert working electrode was molybdenum (or tungsten) wire (Ø1 mm) for the investigation of electrochemical behavior. The lower end of the working electrode was thoroughly polished by SiC paper, and then cleaned in ethanol using the method of ultrasonic cleaning. The active electrode surface was determined after each experiment by measuring the immersion depth of the electrode in the molten salt. For the formation of Mg–Zr alloy, liquid magnesium was used as the working electrode. The liquid magnesium electrode was contained in a small quartz crucible (Ø10 mm) which was placed in an outer corundum crucible. A graphite rod (Ø6 mm) served as a counter electrode. All the experiments were carried out under a carefully purified and dehydrated argon atmosphere.

2.2. Chemicals

The electrochemical behaviors of Zr(IV) were studied in the molten LiCl–KCl–K_2ZrF_6 system. The LiCl–KCl eutectic mixture (LiCl:KCl = 58:42 mol%, reagent grade) was dried under vacuum for more than 72 h at 473 K to remove residual water. Zirconium potassium fluoride was prepared by recrystallization of K_2ZrF_6 (chemically grade) from dilute muriatic acid solution and dried under vacuum at 473 K. In order to remove the residual water and some metal impurities, pre-electrolysis were conducted using a molybdenum electrode at −0.3 V (versus Ag/AgCl) for 5 h in a molten LiCl–KCl–K_2ZrF_6 at temperature of every experiment.

2.3. Electrochemical equipment and techniques

All of the electrochemical studies were performed with IM6e electrochemical workstations (Zahner Co.) and the measurement was controlled by the IM6e software package. Cathode deposits and precipitates were identified by X-ray diffraction (XRD). Scanning electron microscopy (SEM) was used to observe the surface morphology of Mg–Zr alloy. The zirconium concentration in samples was determined by an inductively coupled plasma atomic emission spectrometer (ICP-AES).

3. Results and discussions

3.1. Inert electrode

3.1.1. Cyclic voltammetry

A cyclic voltammetry experiment using a molybdenum working electrode was carried out in the molten LiCl–KCl electrolyte (Fig. 2). There was no significant peak within the potential range of 0 V to −2.4 V (Li^+ reduction) versus the reference electrode-Ag/AgCl in the cyclic voltammogram and the residual current was less than 0.5 mA. This indicated that the reaction of impurities in the system was negligible within the potential range from −2.4 V to 0 V.

In order to investigate the electrochemical behavior of Zr(IV), cyclic voltammetry at various scan rates was conducted in a molten LiCl–KCl–K_2ZrF_6 (added 1.000 mol%) system at 773 K with a molybdenum electrode in the potential range of −1.6 V to 0 V versus the reference electrode – Ag/AgCl (Fig. 3). There were two current peaks in the voltammogram, one is the cathodic current peak and the other one is the anodic current peak. On the cathodic sweep, the current was observed from the voltage approximately −1.40 V, which corresponds to the deposition of Zr metal. After the reversal of sweep direction, an anodic current peak corresponding to the dissolution of the Zr metal was observed at −1.36 V. And there was no significant difference in shape among the voltammograms at various scan rates. However, the cathodic peak shifted a little towards the negative potential with the increase of scan rates which indicated that the reduction process of Zr(IV) may be quasi-reversible [14]. Based on the result of the cyclic voltammograms obtained at molybdenum

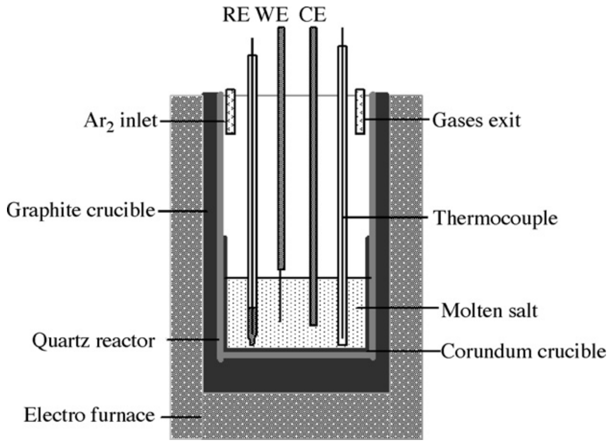

Fig. 1. Apparatus of electrolysis cell.

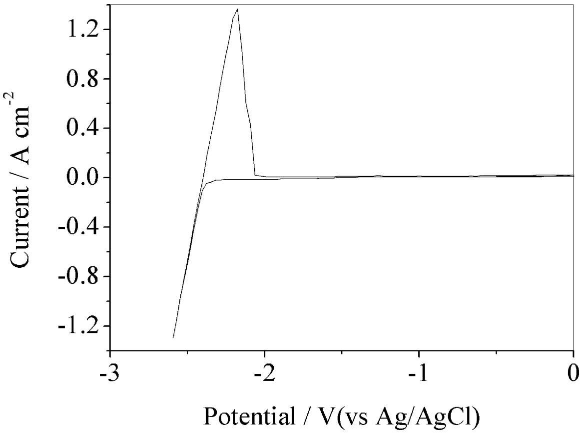

Fig. 2. Cyclic voltammogram for molybdenum electrode in the LiCl–KCl eutectic melt at 773 K. Scan rate = 0.1 V s^{-1}.

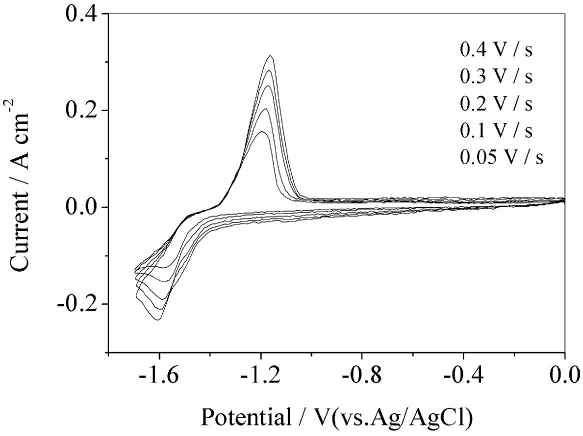

Fig. 3. Cyclic voltammograms at various scan rates for molybdenum electrode in the LiCl–KCl eutectic melt containing 1.000 mol% K_2ZrF_6 at 773 K.

electrode, it seems that the electroreduction of Zr(IV) proceeds via a one step process at 773 K.

For the further investigation of the electrochemical behavior of Zr(IV), cyclic voltammograms were recorded over a potential range from −1.6 V to 0 V (versus Ag/AgCl) at molybdenum electrode in the temperature range 773–973 K (Fig. 4). It could be seen from the voltammograms that the number of cathodic and anodic peaks at 773 K was the same as that at 873 K. However, a new current peak B was observed at 973 K on the cathodic sweep and the peak appeared at −0.67 V. The cathodic peak A was also observed. After the reversal of sweep direction, only the anodic peak A′ corresponding to A was observed. Is there only one oxidation reaction occurred on the anodic sweep? To make this question clear, a cyclic voltammetry experiment with tungsten electrode at the same temperature (973 K) was carried out. The voltammogram is shown in Fig. 5. A small anodic current peak (B′) corresponded to the cathodic peak B was observed. As can be seen from this series of CV measurements, there should exist two couple of redox current peak in the voltammogram for the LiCl–KCl–K_2ZrF_6 melt at 973 K. But the anodic peak (B′) was hidden by the current peak A′ for molybdenum electrode. Based on these experiments, it can be summarized that the number of current peaks on the voltammogram was related to the working temperature. Similar observation was proposed by Baboian et al. [8], Suzuki [9] and Kawase et al. [10].

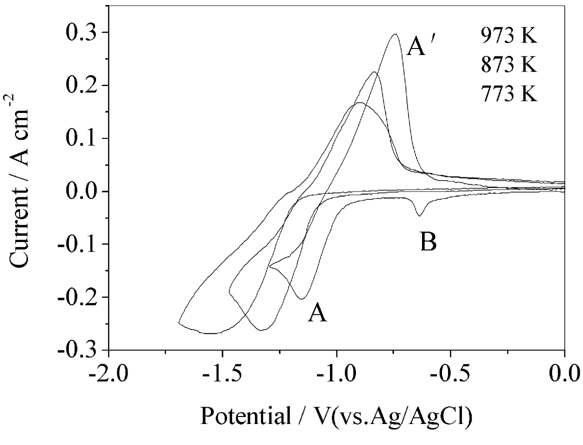

Fig. 4. Cyclic voltammograms at various temperature for molybdenum electrode in the LiCl–KCl eutectic melt containing 1.028 mol% K_2ZrF_6. Scan rate = 0.2 V s^{-1}.

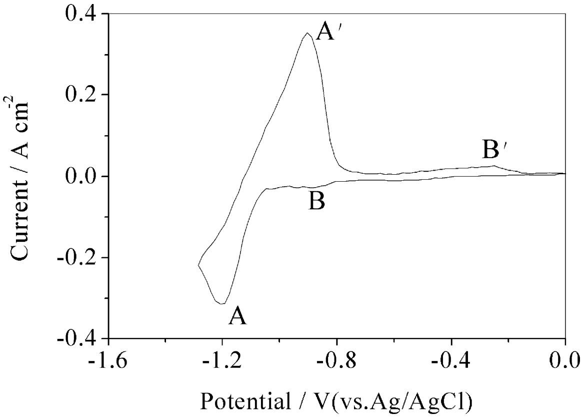

Fig. 5. Cyclic voltammogram for tungsten electrode in the LiCl–KCl eutectic melt containing 1.028 mol% K_2ZrF_6 at 973 K. Scan rate = 0.2 V s^{-1}.

Based on the results of the cyclic voltammograms obtained at molybdenum and tungsten electrodes at 973 K, it was indicated that the electroreduction of Zr(IV) proceeded a two-step process electrolysis. Cathodic peak B is probably related to the reduction of Zr(IV)/Zr(II), which corresponds to the following reaction:

$$\text{Peak(B)}: \quad \text{Zr(IV)} + 2e^- \rightarrow \text{Zr(II)} \tag{1}$$

And cathodic peak A is probably related to the reduction of Zr(II)/Zr, which corresponds to the following reaction:

$$\text{Peak(A)}: \quad \text{Zr(II)} + 2e^- \rightarrow \text{Zr} \tag{2}$$

The anodic peaks A′ and B′ correspond to the oxidation of the Zr metal and Zr(II), respectively:

$$\text{Peak(A}'\text{)}: \quad \text{Zr} \rightarrow \text{Zr(II)} + 2e^- \tag{3}$$

$$\text{Peak(B}'\text{)}: \text{Zr(II)} \rightarrow \text{Zr(IV)} + 2e^- \tag{4}$$

The proposed reduction process of Zr(IV) would be confirmed at the following potentiostaic electrolysis experiment. Because the ratio between Zr(II) and Zr(IV) was low at 773 K and 873 K so that the cathodic peak B might be hidden by the cathodic peak A and would not appear on the corresponding voltammograms. The similar result was also observed by Sakamura [13]. However, Sakamura reported that the Zr(IV) ion was reduced to not only Zr metal and Zr(II) but also Zr(I) in a molten LiCl–KCl–$ZrCl_4$ system. This discrepancy might be ascribed to the different chemical systems.

3.1.2. Chronopotentiogram

Chronopotentiometry was carried out to further investigate the electroreduction process of Zr(IV). A typical chronopotentiogram for the electroreduction of Zr(IV) to Zr in LiCl–KCl eutectic is shown in Fig. 6. The experiment was carried out at molybdenum electrode with a current density of 0.139 A cm^{-2} at 973 K.

Two potential plateaus were seen in the potential range from −1.25 V to −0.6 V in the chronopotentiogram corresponding to

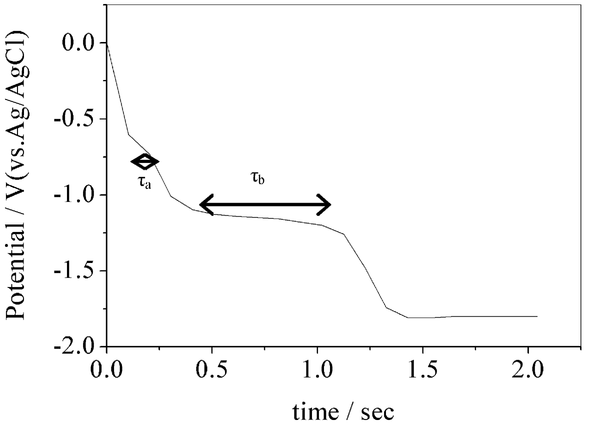

Fig. 6. Chronopotentiogram for molybdenum electrode in LiCl–KCl eutectic melt containing 1.028 mol% K_2ZrF_6 at 973 K. Current density = 0.139 A cm^{-2}.

two reduction processes. The potential τa and τb corresponded to the cathodic peak B and A of the cyclic voltammograms, respectively. After the second plateau, there was a rapid decrease of the potential and the electrode potential reaches a limiting value corresponding to the deposition of the lithium metal. The results of chronopotentiometry further confirmed that the electroreduction of Zr(IV) proceeded via a two step process.

3.2. Magnesium electrode

For the preparation of Mg–Zr alloy, a liquid magnesium electrode was used. The cyclic voltammograms for liquid magnesium electrode before and after adding K_2ZrF_6 into the LiCl–KCl melt were shown in Figs. 7 and 8, respectively. Before adding K_2ZrF_6, one cathodic current was observed at −2.0 V which should correspond to the electrochemical formation of a Li–Mg alloy. On the anodic sweep, two anodic current peaks were observed. The anodic current peak at −2.0 V contributed to Li dissolution from Li–Mg alloy. The other current peak (C′) at −1.3 V should be associated with the dissolution of Mg.

After adding K_2ZrF_6, the cathodic peak A thought to be caused by the formation of Mg–Zr alloy was observed at −1.32 V (versus Ag/AgCl). The anodic peak A′ corresponded to Zr dissolution from the Mg–Zr alloy was observed at −0.69 V (versus Ag/AgCl). At this potential, the dissolution of Mg will also occur. But the dissolution current of Mg was so small that this current peak will be hidden by the anodic peak A′. On the other hand, because the anodic dissolution potential of Mg is more negative than that of Zr, Zr(IV) and Zr(II) ions might be reduced spontaneously by Mg metal in this melt. Therefore, the mechanism of the formation of Mg–Zr alloy are considered that: (i) Zirconium is electrodeposited on the magnesium electeode, and (ii) Zr(IV) and Zr(II) ions are reduced by Mg metal.

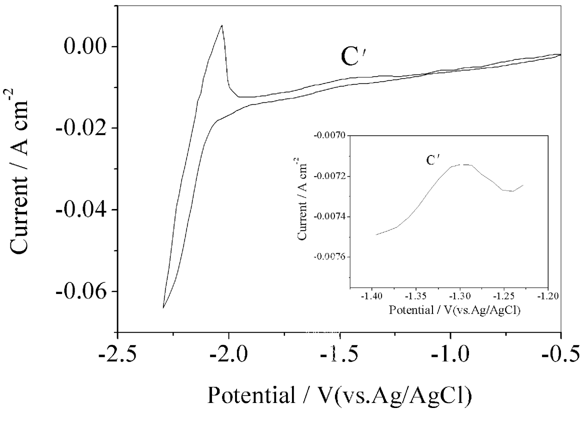

Fig. 7. Cyclic voltammogram at 0.05 V s^{-1} scan rates for liquid magnesium electrode in the LiCl–KCl eutectic melt at 973 K.

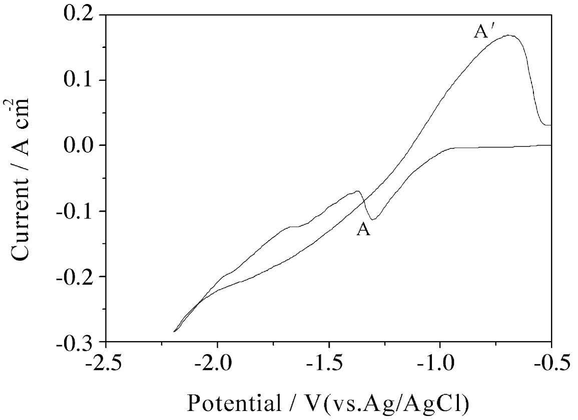

Fig. 8. Cyclic voltammogram at 0.05 V s^{-1} scan rates for liquid magnesium electrode in the LiCl–KCl eutectic melt containing 1.028 mol% K_2ZrF_6 at 973 K.

3.3. Potentiostatic electrolysis

3.3.1. Molybdenum electrode

In order to confirm the electroreduction products of Zr(IV), potentiostatic electrolysis experiments were conducted at 973 K, and controlled potential electrolysis was carried out using a molybdenum electrode at −0.75 V and −1.25 V (versus Ag/AgCl) which were selected based on the results of cyclic voltammetry and chronopotentiometry. The detailed test conditions and results were shown in Table 1. During the potentiostatic electrolysis of test 1 and test 2, a part of the products deposited at the molybdenum electrode and the other part of products deposited at the bottom of the corundum crucible. After the electrolysis, the sample with a mass of salt was washed by distilled water and dried under vacuum at 333 K. The XRD pattern of the gray powder sample 1 obtained at −0.75 V is shown in Fig. 9. The gray powder was identified as $ZrCl_2$. The XRD pattern of the black powder sample 2 obtained at −1.25 V is shown in Fig. 10. The sample 2 was identified as a mixture of Zr and $ZrCl_2$. Combining the potentiostatic electrolysis and XRD analysis, the

Table 1
Test conditions and results for cathode deposition in LiCl–KCl eutectic containing K_2ZrF_6

Sample no.	$X_{K_2ZrF_6}$	Current (mA)	Cathode	Potential (V vs. Ag/AgCl)	Product
1	0.01028	10–15	Mo	−0.75	$ZrCl_2$
2	0.01028	40–50	Mo	−1.25	Zr and $ZrCl_2$
3	0.01028	42–53	Mg	−1.30	Mg–Zr alloy

$X_{K_2ZrF_6}$ mole fraction of K_2ZrF_6 in LiCl–KCl eutectic.

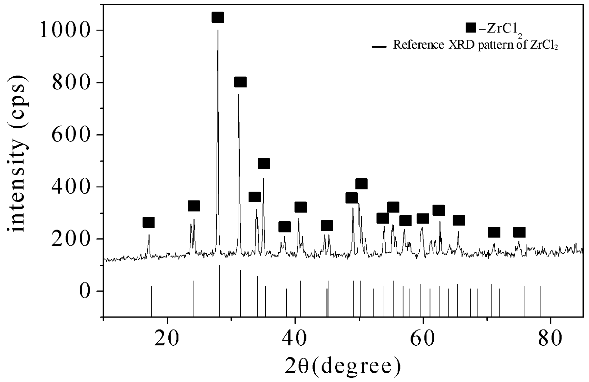

Fig. 9. XRD patterns of the sample obtained at molybdenum electrode under potentiostatic electrolysis at −0.75 V vs. Ag/AgCl.

result further showed that the Zr(IV) was reduced to Zr metal by a two-step mechanism corresponding to the Zr(IV)/Zr(II) and Zr(II)/Zr transitions. It was in good agreement with the result of cyclic voltammetry and chronopotentiometry.

3.3.2. *Magnesium electrode*

For the preparation of Mg–Zr alloy, potentiostatic electrolysis experiments were conducted using a liquid magnesium electrode at −1.3 V (versus Ag/AgCl). The detailed test conditions and results were shown in Table 1. After the electrolysis, the sample with a mass of salt was washed by anhydrous ethylene glycol and stored inside a glove box. The surface morphology of Mg–Zr alloy was observed by scanning electron microscopy (SEM) (Fig. 11). In the SEM pattern, the heterogeneous nucleus (A) can be seen. The corresponding EDX analysis (Fig. 12) shows that the heterogeneous nucleus (A) consists of zirconium and magnesium. The content of zirconium was about 9.91 mass%. By ICP-AES analysis, the zirconium concentration in the sample of Mg–Zr was about 0.8 mass%. Low Zr concentration was caused primarily by lower solid solubility of zirconium in the magnesium. However, Zr has a better effect on the refining of crystal grains and improving of mechanical properties of magnesium alloys when the content of zirconium is 0.6–0.8 mass% [15]. Therefore, the obtained Mg–Zr alloy in this experiment can fulfill the demand of applications.

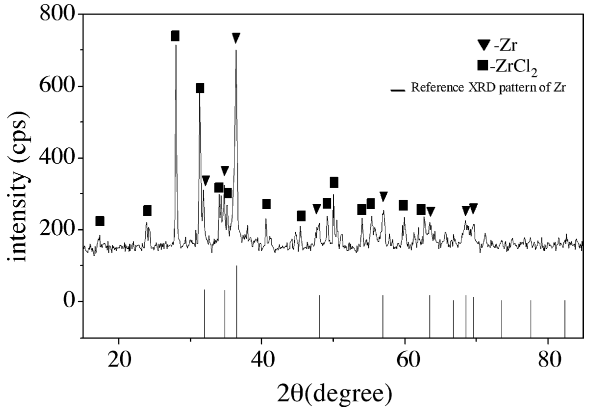

Fig. 10. XRD patterns of the sample obtained at molybdenum electrode under potentiostatic electrolysis at −1.25 V vs. Ag/AgCl.

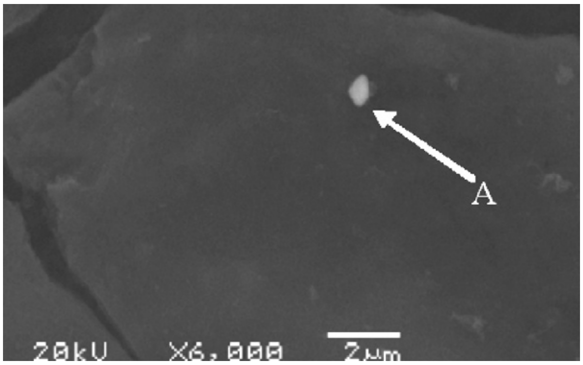

Fig. 11. SEM images of the Mg–Zr alloy nucleus formed by potentiostatic electrolysis at −1.3 V vs. Ag/AgCl for 1 h.

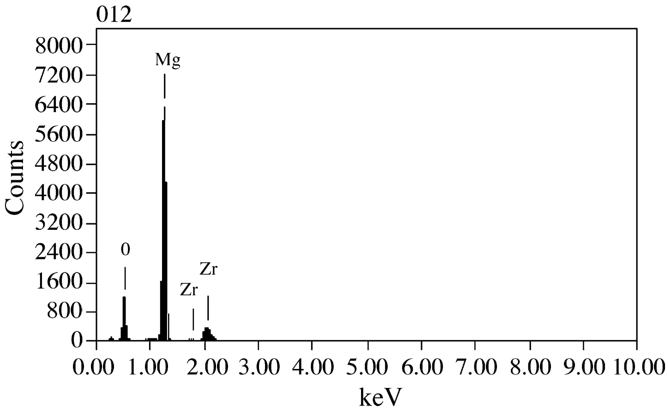

Fig. 12. EDX of the Mg–Zr alloy nucleus formed by potentiostatic electrolysis at −1.3 V vs. Ag/AgCl for1 h.

4. Conclusions

The electrochemical behavior of Zr(IV) was studied in the eutectic LiCl–KCl mixture at different substrates (Mo, W and liquid Mg) by various electrochemical techniques. The cyclic voltammetry and chronopotentiometry results showed that Zr(IV) was reduced to Zr metal by a two-step mechanism in the LiCl–KCl–K_2ZrF_6 melt. The intermediate product was $ZrCl_2$ identified by XRD analysis, and the ratio between Zr(II) and Zr(IV) became larger with the increase of temperature.

The Mg–Zr alloy was prepared at the liquid magnesium electrode at −1.3 V (versus Ag/AgCl) by potentiostatic electrolysis. The content of zirconium was about 9.91 mass% of the erogeneous nucleus and the zirconium concentration of the whole Mg–Zr alloy was about 0.8 mass%.

Acknowledgements

The authors wish to extend thanks to professors D.Y. Qiu and L.Y. He for their interest and useful suggestions.

References

[1] B.K. Xiong, X.M. Yang, F.C. Luo, The Application of Zirconium, Hafnium and their Compounds, Metallurgical Industry Press, Beijing, 2002, pp. 170–240.

[2] Q. Ma, M.T. Frost, Scripta Mater. 46 (2002) 649.

[3] Z.H. Lin, Handbook of Refinement and Metallurgy of Nonferrous Metal, Metallurgical Industry Press, Beijing, 1999, pp. 111–128.

[4] G.Z. Chen, D.J. Fray, T.W. Farthing, Nature 407 (2000) 361.

[5] T. Nohira, K. Yasuda, Y. Ito, Nat. Mater. 2 (6) (2003) 397.

[6] L.P. Polyakova, P. Taxil, E.G. Polyakov, J. Alloys Compd. 359 (2003) 244.

[7] A.M. Martinez, Y. Castrillejo, B. Børresen, et al., J. Electroanal. Chem. 493 (2000) 1.

[8] R. Baboian, D.L. Hill, R.A. Bailey, J. Electrochem. Soc. 112 (1965) 1221.

[9] T. Suzuki, Denki Kagaku 39 (1971) 864.

[10] M. Kawase, Y. Ito, J. Appl. Electrochem. 33 (2003) 785.

[11] F. Basile, E. Chassaing, G. Lorthioir, J. Appl. Electrochem. 11 (1981) 645.

[12] G.J. Kipouros, S.N. Flengas, J. Electrochem. Soc. 132 (1985) 1087.

[13] Y. Sakamura, J. Electrochem. Soc. 151 (2004) C190.

[14] A.J. Bard, L.R. Faulkner, Electrochemical Methods, Fundamentals and Applications, Wiley, New York, 1980.

[15] Z.H. Chen, Magnesium Alloy, Chemical Industry Press, Beijing, 2004, p. 53.